

Modeling Principles Using the Relation Between Lagrange Multipliers and Bond Graphs

José J. Granda
Professor
California State University,
Sacramento.
Mechanical Engineering
Sacramento, California, 95819
grandajj@ecs.csus.edu

Louis Nguyen
NASA Johnson Space Center
Integrated Navigation,
Guidance
and Control Analysis Branch,
Houston, TX 77058
louis.h.nguyen@nasa.gov

Paul Brocker
Graduate Student
California State University,
Sacramento
Mechanical Engineering
Sacramento, California, 95819
psbrocker@gmail.com

I. ABSTRACT

Modeling dynamic systems by bond graphs has become state of the art technology since hundreds of researchers around the world have incorporated the technology in many fields of engineering and science. The legacy of its inventor Prof. Henry Paynter at MIT in 1959 is now a fundamental and practical technique to understand reality by building computer models. This paper addresses a particular aspect of this technology when modeling of mechanical systems requires relaxation of constraints by means of Lagrange principles. Lagrange's equations are a useful means of describing and solving systems with kinematic constraints. Lagrange multipliers are variables used in equations to find the extremes of multivariate functions. Here we explore the relation of Lagrange multipliers to solve modeling difficulties of a space vehicle with equations with dependent derivatives. Lagrange multipliers were used in conjunction with bond graphs to simulate a system where joints of kinematic linkages produce dependent derivatives. NASA's Morpheus Project lunar lander was used as a case study. The Morpheus Project is a terrestrial test vehicle designed to fly the terminal descent trajectory of a lunar lander to advance the Autonomous Landing Hazard Avoidance Technology (ALHAT). An objective of this study is to apply the modeling approach herein to capture the dynamic movement of the lander as the propellant is sloshed and consumed. This paper expands further the analysis presented by [1] (Granda, J J. Nguyen, L, Carlson, T, Sahragard-Monfared, G., Fornalski, E., Brocker 2016). Using an automated approach bond graph models of state space equations were generated using the Computer Aided Modeling Program (CAMPG). Integral causality models and derivative

causality models were considered in order to find the simpler solution for the mathematical dependencies produced in modeling this vehicle.

Author Keywords:

Derivative causality, Lagrange Multipliers, Bond Graph Models, Morpheus vehicle, CAMPG, MATLAB, SIMULINK.

II INTRODUCTION

The basic model to analyze the propellant slosh and consumption of the lander vehicle is a double pendulum, which represents the lander vehicle (and tanks) hanging under tether along with pendulum masses for the propellant (fuel and oxidizer). Fig. 1 gives us an idea of the Morpheus vehicle.

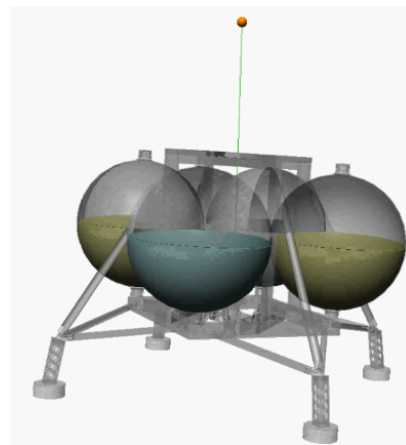


Fig. 1 Morpheus vehicle. Two methane and two oxygen tanks.

Systems in which the movement of “particles” is of interest can be analyzed with Lagrange equations. “Lagrange Multipliers” can be used to describe a system of equations with constraints. To get from the diagram of the double pendulum integral causality bond graph to the equations used for the bond graph in this paper, Lagrange multipliers were used.

Using the software Working Model 2-D, a two dimensional kinematic model was developed for the lander. A vector model was obtained using a two dimensional representation of a double pendulum. CAMPG [2] (Cadsim Engineering 2018) was used for the bond graph and for generating the equations of motion whether in integral or derivative form.

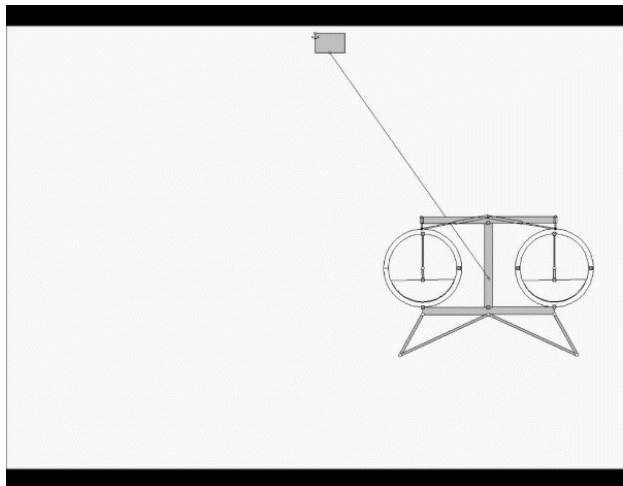


Fig. 2 Lander-fuel slosh model two-dimensional pendulum model. Working Model 2-D

III Analysis and Model Development

A. Single Pendulum and Proof of Concept

Before we try the double pendulum, let us establish and verify the operation using a single pendulum model.

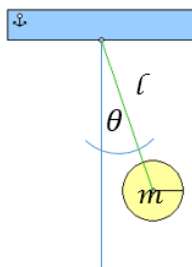


Fig. 3 Single pendulum model

$$\sum M = I\ddot{\theta} \tag{1}$$

$$mg \sin \theta * r = mr^2\ddot{\theta} \tag{2}$$

A Simulink model may be generated from this equation. The following model was constructed by taking a summation block with one input and one output, two gains, two integral blocks, a sine block, to represent the equation in graphical form.

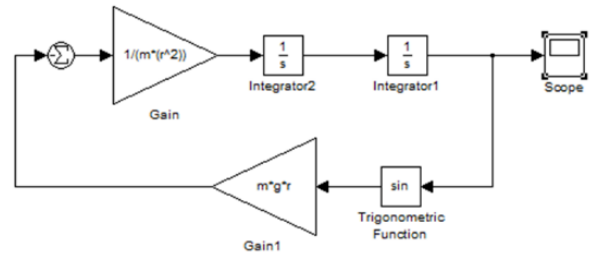


Fig. 4 Simulink Block Diagram Model

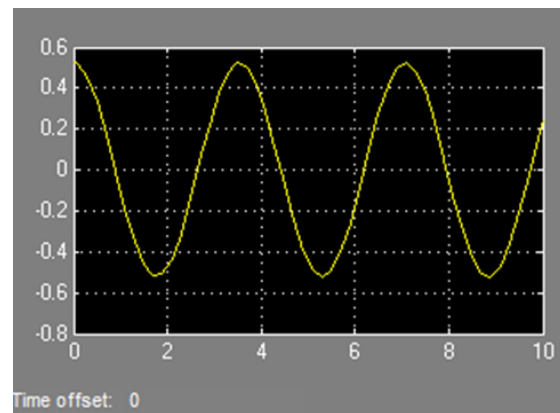


Fig. 5 Simulink model output test

Now let us try for comparison a bond graph model of the same system as the one shown in Fig. 6. The mass is an I element, gravity an effort source, and the conservative, spring-like “swinging motion” by a capacitor element.

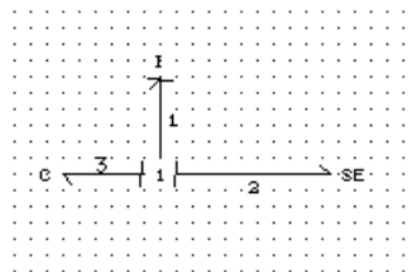


Fig. 6 Bond Graph model of single pendulum model

This demonstrates the equivalence of the block diagram method compared to a computer-generated model from CAMPG/MATLAB using bond graphs. The first one required a free body diagram, the second did not. It required only to establish the kind of elements the system is composed and how are they interconnected. This demonstrates the equivalence. The following graph is the step response, which produces the exact same result.

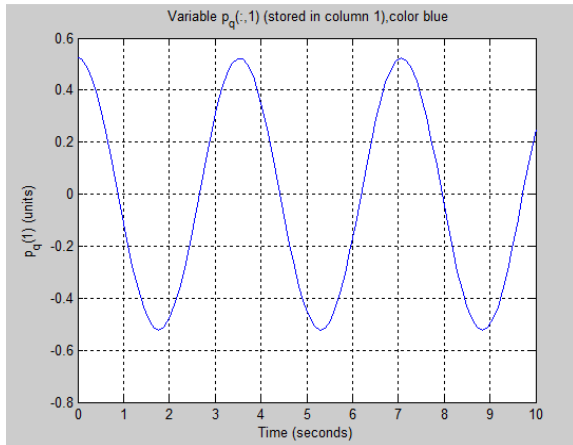


Fig. 7 Bond graph output

This output is the same as the Simulink model. This verifies the method and proves it reliable.

We may also demonstrate that the two models are actually equivalent. If we construct a second block diagram based on the bond graph equations generated from CAMPG, we can show it to be equivalent to the original Simulink model through the following steps.

The Simulink model based on the bond graph equations is shown below. “I” element is represented by the integrator and the gain at the top. The integrator, sine, and gain block to the left and by the constant block to the right represent the “C”. The scope is placed between the sine block and the integrator to obtain the output for the angular displacement.

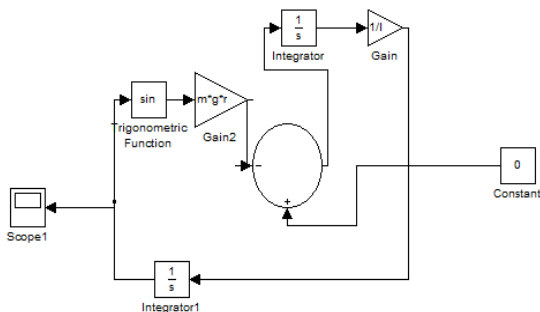


Fig. 8 Initial state Simulink Model

Several rearrangements of the block diagram will lead us to the equivalence of the two models started with different approaches. The constant is removed and the summation block is adjusted. It has only one input and one output (the same as the remaining number of branches). The elements on the left side of the summation block are dragged around to the right side. This is done in order to begin to lay out the model in the same orientation as the Simulink model based on the second order pendulum equation.

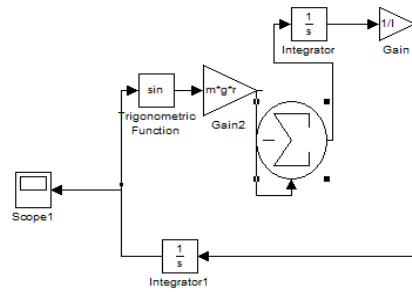


Fig. 9 Simulink model after first rearrangement.

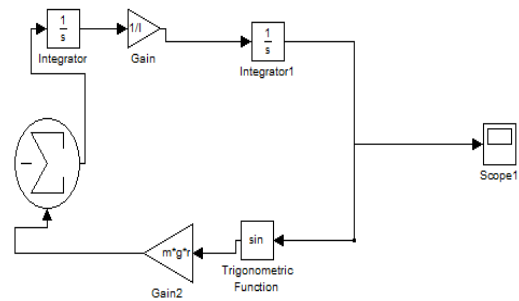


Fig. 10 Simulink model after second rearrangement

Finally, the gain is taken and moved to the left of the first integrator without changing its value.

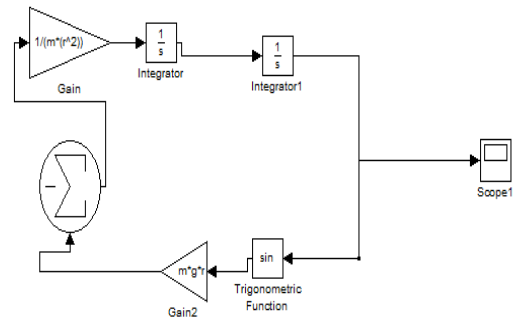


Fig. 11 Simulink model after third rearrangement.

This is exactly equivalent to the block diagram shown in Fig. 4.

Having shown that the model that started with the bond graph and the one that started with the block diagram approach after derivation of equations using a free body diagram produce the same results, the conclusion is that the two models are in fact equivalent. Using that principle, a double pendulum model is then developed.

B. Two degrees of freedom model

Let us examine the model presented in [6] (Yehia A. Khulief 1991) and apply our approach. They solved a similar problem using the Lagrange equations used in conjunction with bond graphs. Khulief gives an example of a simple spring-mass connected pendulum, in addition to giving a detailed step based method for using and applying Lagrange equations and Bond graphs conjointly.

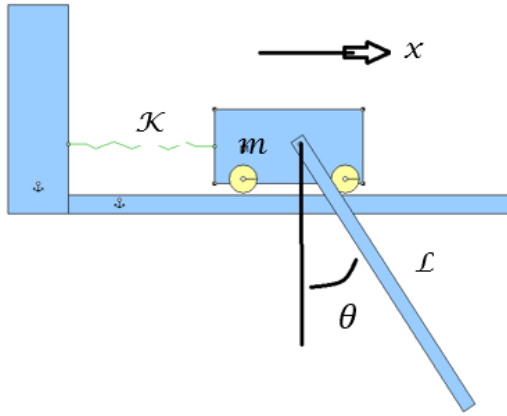


Fig. 12 Movable pendulum with spring

Yehia Khulief [6] first define the x and y equations in order to find the constraints for the system.

$$x = X + L\sin\theta \text{ and } y = L\cos\theta \quad (3)$$

Differentiating in order to find the MTF equations:

$$\dot{x} = \dot{X} + (L\cos\theta)\dot{\theta} \text{ and } \dot{y} = -(L\sin\theta)\dot{\theta} \quad (4)$$

The state equations for the two state variables are:

$$\dot{p}_1 = -\dot{p}_2 - e_5 \quad (5)$$

$$\dot{p}_4 = m_r g L \sin\theta - (L\cos\theta)\dot{p}_2 + (L\sin\theta)\dot{p}_3 \quad (6)$$

Another two equations are obtained by taking the flow expressions in conjunction with the element relations and differentiating:

$$\dot{p}_2 = \left(\frac{m_r}{M}\right)\dot{p}_1 + \left[\frac{m_r L \cos\theta}{I_G}\right]\dot{p}_4 - \left[\frac{m_r L \sin\theta}{I_G^2}\right]p_4^2 \quad (7)$$

$$\dot{p}_3 = -\left[\frac{m_r L \sin\theta}{I_G}\right]\dot{p}_4 - \left[\frac{m_r L \cos\theta}{I_G^2}\right]p_4^2 \quad (8)$$

Equations of motion with constraints from \dot{p}_2 and \dot{p}_3 .

$$(M + m_r)\ddot{X} + KX + (m_r L \cos\theta)\ddot{\theta} - (m_r L \sin\theta)\dot{\theta}^2 = 0$$

$$(I_G + m_r L^2)\ddot{\theta} + (m_r L \cos\theta)\ddot{X} + m_r g L \sin\theta = 0 \quad (9)$$

The bond graph for the system is:

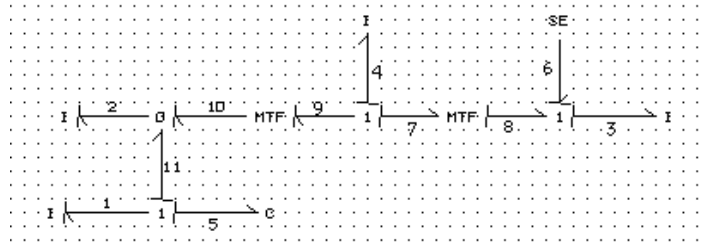


Fig. 13 Mobile pendulum bond graph

The potential energy equation:

$$T = \frac{1}{2}(M + m_r)\dot{X}^2 + \frac{1}{2}(I_G + m_r L^2)\dot{\theta}^2 + (m_r L \cos\theta)\dot{\theta}X \quad (10)$$

The forces are then:

$$Q_\theta = -m_r g L \sin\theta, \text{ and } Q_x = -KX \quad (11)$$

The Lagrangian forms are then finally:

$$\frac{d}{dt}\left\{\frac{\partial T}{\partial \dot{X}}\right\} - \left\{\frac{\partial T}{\partial X}\right\} - Q_x = 0 \quad (12)$$

$$\frac{d}{dt}\left\{\frac{\partial T}{\partial \dot{\theta}}\right\} - \left\{\frac{\partial T}{\partial \theta}\right\} - Q_\theta = 0 \quad (13)$$

Using these derivations of the Lagrange equations helps us establish the relations that we can use to relate them to bond graph modeling. Therefore, bond graphs models and Lagrange equations can be used to complete the necessary modeling and subsequent simulations.

C. Block Diagram Double Pendulum Models

A double pendulum can be described by two second order, coupled differential equations using free body diagram as presented in [9] (Seto W., 1964).

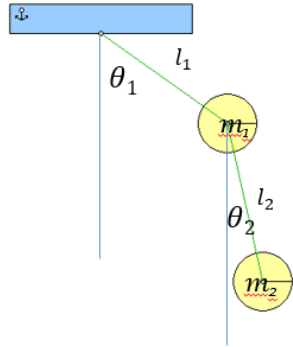


Fig. 14 Double pendulum model

$$m_2 * r_2^2 * \ddot{\theta}_2 = -m_2 * g * r_2 * \sin \theta_2 - m_2 * r_1 * r_2 * \ddot{\theta}_1 \quad (14)$$

$$m_1 * r_1^2 * \ddot{\theta}_1 = -m_1 * g * r_1 * \theta_1 - m_2 * g * r_1 * \theta_1 - m_2 (r_1 * \ddot{\theta}_1 + r_2 * \ddot{\theta}_2) r_1 \quad (15)$$

A Simulink model was developed with these two equations. Taking a summation block with two inputs and one output, two gain blocks, two integrator blocks, a sine block and a scope the first “loop” (the basis of the first equation) can be constructed.

The second equation is constructed taking a summation block with four inputs and one output, four gain blocks, two integrator blocks, and a scope. The block diagram is completed by taking a branch from between the gain and the first integrator block on the first loop and connecting it to a gain block and to the summation block in the second loop. A connection is necessary from between the first gain and the first integrator block on the second loop and connecting it through a gain block to the summation block in the first loop. These last two steps are to account for the $\ddot{\theta}_2$ term in the second equation and the $\ddot{\theta}_1$ term in the first equation.

This block diagram represent two-second order differential equations and thus there are four integrators. When block diagrams are built from the bond graph, single integrators are used for each derivative.

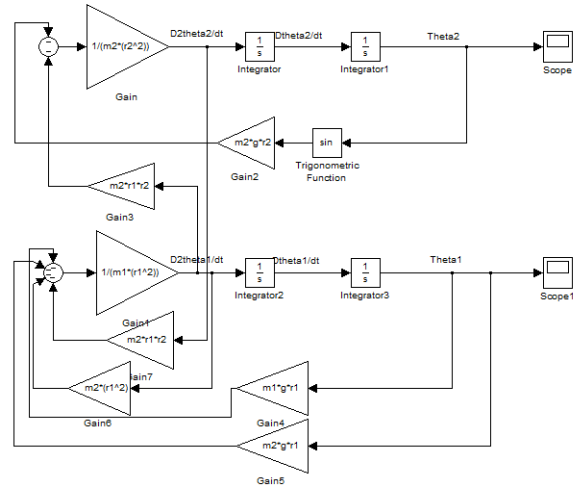


Fig. 14 Simulink model of a double pendulum

The angular position of both “bobs” may be observed as output from the scopes. This yields the following sinusoidal output (for the first and second bob respectively):

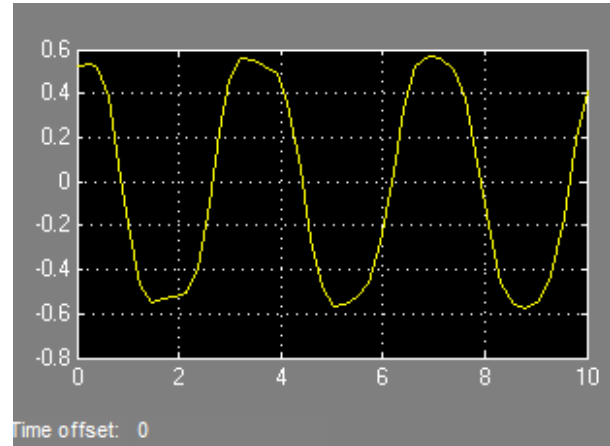


Fig. 15 (a) Bob displacement

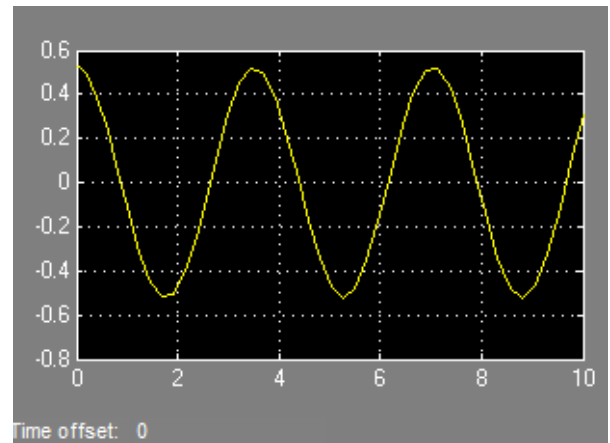


Fig. 15 (b) Second bob displacement.

D. Working Model 2-D Double Pendulum Models

The double pendulum concept was verified using yet another multibody approach, the software Working Model 2-D. This verified the free body diagram models with those developed with bond graphs. The software Working Model 2-D allows the simulation by computing the equations numerically using a multibody approach. The two bob pendulum model was developed in order to establish the fundamental geometry of the vehicle and the fuel inside, which is the basis for the model presented for the Morpheus Project presented in Fig. 1. Working Model 2-D allows the display of the positions, velocity and accelerations of each bob.

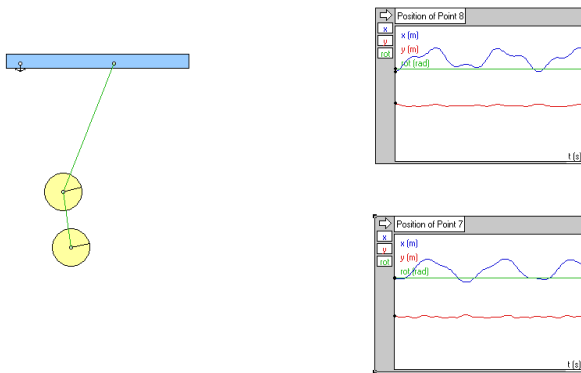


Fig. 16 Working Model 2-D double pendulum model.

The results shown were compared to the output of the block diagram approach and the bond graph approach obtaining similar results.

IV. THREE DIMENSIONAL BOND GRAPH MODELS USING LAGRANGE MULTIPLIERS

A 3-D, untethered model was created using the same process as the 2-D. the following steps shown previously. Using the principles presented in [3] (Karnopp, Margolis, Rosenberg, 2012), a three-dimensional model was developed. We used the artificial infinitesimal displacements δ 's and λ 's to relax the constraints and allow the use of Lagrange multipliers to solve derivative causality.

This diagram shown in Fig. 17 illustrated the three-dimensional set up. We considered the pendulum lengths, masses and angles with the nomenclature of Fig. 14, but with the additional angles and displacements λ 's and δ 's to account for six degrees of freedom. A difference from the 2-D, this now includes a third " λ " and " δ " at each of the connection points, as well as four " φ " angles as illustrated in Fig. 18. This gives us six λ 's and six δ 's and four " φ "'s. In addition, the model is untethered, allowing forces in the x, y, and z direction to act at the origin. The next step is to generate equations describing the system in terms of the deltas, in the same manner it was done with the 2-D model.

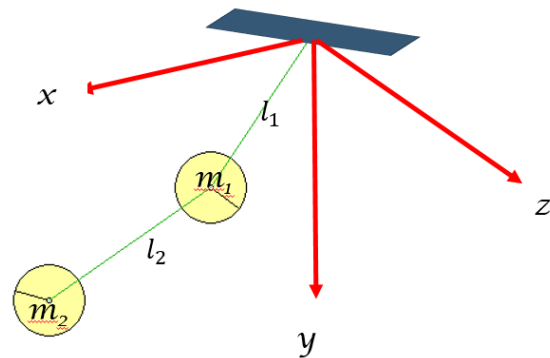


Fig. 17 Three-dimensional model.

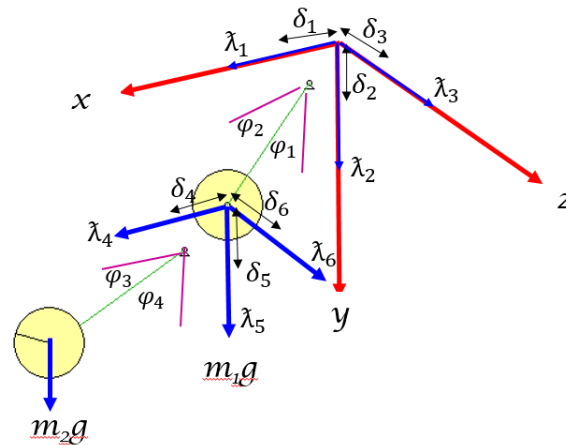


Fig. 18 3-D double pendulum diagram with relaxed constraints to allow the use of Lagrange multipliers.

$$\begin{bmatrix} \dot{\delta}_1 \\ \dot{\delta}_2 \\ \dot{\delta}_3 \\ \dot{\delta}_4 \\ \dot{\delta}_5 \\ \dot{\delta}_6 \end{bmatrix} = \begin{bmatrix} -1 & 1 & 0 & 0 & 0 & 0 & 0 & 0 & 0 & -l_1 \cos \varphi_1 & 0 & 0 & 0 \\ 0 & 0 & 0 & -1 & 1 & 0 & 0 & 0 & 0 & l_1 \sin \varphi_1 & 0 & 0 & 0 \\ 0 & 0 & 0 & 0 & 0 & 0 & -1 & 1 & 0 & 0 & l_1 \sin \varphi_2 & 0 & 0 \\ 0 & -1 & 1 & 0 & 0 & 0 & 0 & 0 & 0 & 0 & 0 & -l_2 \cos \varphi_3 & 0 \\ 0 & 0 & 0 & 0 & -1 & 1 & 0 & 0 & 0 & 0 & 0 & l_2 \sin \varphi_3 & 0 \\ 0 & 0 & 0 & 0 & 0 & 0 & 0 & -1 & 1 & 0 & 0 & 0 & l_2 \sin \varphi_4 \end{bmatrix} \begin{bmatrix} \dot{X} \\ \dot{X}_1 \\ \dot{X}_2 \\ \dot{Y} \\ \dot{Y}_1 \\ \dot{Y}_2 \\ \dot{Z} \\ \dot{Z}_1 \\ \dot{Z}_2 \\ \dot{\phi}_1 \\ \dot{\phi}_2 \\ \dot{\phi}_3 \\ \dot{\phi}_4 \end{bmatrix}$$

Fig. 19 Kinematic relations for development of the three dimensional model

$$\begin{bmatrix} F_X \\ F_{X_1} \\ F_{X_2} \\ F_Y \\ F_{Y_1} \\ F_{Y_2} \\ F_Z \\ F_{Z_1} \\ F_{Z_2} \\ \tau_1 \\ \tau_2 \\ \tau_3 \\ \tau_4 \end{bmatrix} = \begin{bmatrix} -1 & 0 & 0 & 0 & 0 & 0 \\ 1 & 0 & 0 & -1 & 0 & 0 \\ 0 & 0 & 0 & 1 & 0 & 0 \\ 0 & -1 & 0 & 0 & 0 & 0 \\ 0 & 1 & 0 & 0 & -1 & 0 \\ 0 & 0 & 0 & 0 & 1 & 0 \\ 0 & 0 & -1 & 0 & 0 & 0 \\ 0 & 0 & 1 & 0 & 0 & -1 \\ 0 & 0 & 0 & 0 & 0 & 1 \\ -l_1 \cos \varphi_1 & l_1 \sin \varphi_1 & 0 & 0 & 0 & 0 \\ 0 & 0 & l_1 \sin \varphi_2 & 0 & 0 & 0 \\ 0 & 0 & 0 & -l_2 \cos \varphi_3 & l_2 \sin \varphi_3 & 0 \\ 0 & 0 & 0 & 0 & 0 & l_2 \sin \varphi_4 \end{bmatrix} \begin{bmatrix} \lambda_1 \\ \lambda_2 \\ \lambda_3 \\ \lambda_4 \\ \lambda_5 \\ \lambda_6 \end{bmatrix}$$

Fig. 20 Force-Torque relations

The new relaxed constraints yield the following six λ 's equations (17) to (21). Their derivatives are summarized in matrix form.

$$\delta_1 = x_1 - x - l_1 \sin \varphi_1 \quad (16)$$

$$\delta_2 = y_1 - y - l_1 \cos \varphi_1 \quad (17)$$

$$\delta_3 = Z_1 - Z - l_1 \cos \varphi_2 \quad (18)$$

$$\delta_4 = x_2 - l_2 \sin \varphi_3 - x_1 - l_1 \sin \varphi_1 \quad (19)$$

$$\delta_5 = y_2 - l_2 \cos \varphi_3 - y_1 - l_1 \cos \varphi_1 \quad (20)$$

$$\delta_6 = Z_2 - l_2 \cos \varphi_4 - Z_1 - l_1 \cos \varphi_1 \quad (21)$$

The derivatives of these six equations are taken to give the six $\dot{\delta}$'s, which will become the six left-side derivatives represented in the bond graph. The

equations are then expressed in matrix and shown on Fig. 19. If we look at these transformation that relates linear velocities for the Lagrange relaxation variables to linear and angular velocities of interest in the double pendulum in three dimensions we realize these correspond to the MTF elements (Multiport Transformers).

The matrix transformation relates the $x, y, z, \varphi_1,$ and φ_2 motion to the $\dot{\delta}$'s. This includes $X, Y,$ and Z forces at the origin and in the joints.

Knowing that multiport transformers, MTF's carry the inherent advantage to yield the set of equations for the forces and the torques, then it follows that using the matrix equations we obtain those that relate the Forces and the Torques to the Lagrange lambda variables as shown in the matrix transformation of Fig. 20.

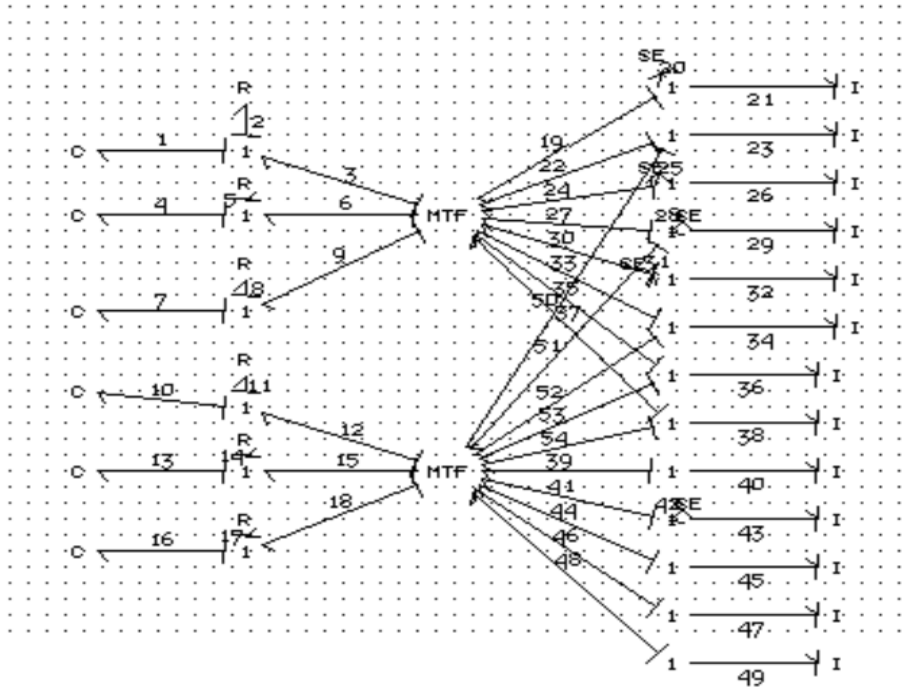


Fig. 21 CAMPG, three dimensional pendulum bond graph

The multiport transformers relate the forces and torques to the six λ 's forces. The next step is to generate the bond graph based on these transformation equations. There are six branches on the left side with six "1" junctions, six capacitive elements, and six resistive elements. There are two transformers, one for each of the two "bobs." As can be seen from the matrices, there will now be thirteen inertial elements on the right side. Those which represent inertia in the "y" direction are assigned effort sources at their "1" junctions because of gravity. Then, judging by the dynamic equations (not pictured) it can be determined that the "X" branch should be connected to only the first transformer element, the "X₁" branch should be connected to the first and second transformer elements, the "y" branch should only be connected to the first transformer element, and so on. Effort sources (or SE's) are attached to the inertial elements, which correspond to motion in the y direction. Following these steps, the bond graph is obtained as shown in Fig. 21.

The next step is to export the bond graph model equations to MATLAB. CAMPG does this by producing .m files that contain the parameters of the system, the simulation time, the desired output variable and the differential equations of the system in explicit form. The solution presented here using the Lagrange multipliers produces a model with integral causality and therefore an explicitly set of equations. The transformer values are calculated as trigonometric

expressions. Then λ 's the δ 's are calculated solving the system of differential equations and forces and torques are calculated by their respective e's outputs. For example, F_x is e19 and λ_1 is e3. The transformer expressions are described the output displacement and forces specified. Once all the known physical parameter values are entered, the time or frequency domain simulation can take place. Fig. 22 is an example.

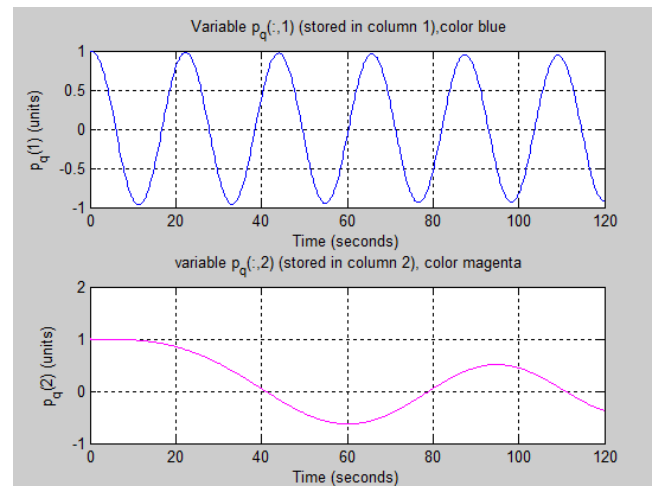


Fig. 22 Output displacements of the bobs from the 3-D double pendulum bond graph.

V. THE DERIVATIVE CAUSALITY CASE

If no relaxation of the constraints is present the model is a 3-D model with derivative causality and therefore with a set of implicit equations. That alternative and its proposed solution is presented here.

The derivative causality model has six angles and six velocity components. This leads to the derivation of six equations. [9] (Fitzpatrick, 2011) presents a single bob spherical pendulum. Here a double spherical pendulum and its bond graph are developed based on the kinematic relations.

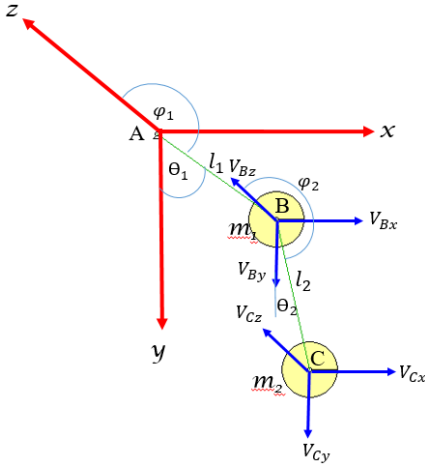


Fig. 23 Derivative causality model.

$$V_A = 0 \quad (22)$$

$$V_B = V_A + \omega_{AB} x r_{B/A} \quad (23)$$

$$r_{B/A} = (l_1 \sin \theta_1 \cos \varphi_1) i - (l_1 \sin \theta_1 \sin \varphi_1) j + (l_1 \sin \theta_1) k \quad (24)$$

$$\omega_{AB} = \omega_2 \sin \varphi_1 i - \omega_2 \cos \varphi_1 j + \omega_1 k$$

$$\omega_{AB} x r_{B/A} = \begin{vmatrix} & i & j & k \\ \omega_2 \sin \varphi_1 & & & \omega_1 \\ l_1 \sin \theta_1 \cos \varphi_1 & l_1 \sin \theta_1 \sin \varphi_1 & l_1 \sin \theta_1 & \end{vmatrix}$$

$$= (-\omega_2 \cos \varphi_1 i (l_1 \sin \theta_1)) - (\omega_1 (l_1 \sin \theta_1 \sin \varphi_1)) i - (\omega_2 \sin \varphi_1 (l_1 \sin \theta_1)) - \omega_1 l_1 \sin \theta_1 \cos \varphi_1 + ((\omega_2 \sin \varphi_1 (l_1 \sin \theta_1 \sin \varphi_1)) - \omega_2 \cos \varphi_1 l_1 \sin \theta_1 \cos \varphi_1) k \quad (25)$$

$$\begin{aligned} V_{Bx} &= (\omega_2 (l_1 \cos \theta_1) \cos \varphi_1) + l_1 \omega_1 \sin \theta_1 \sin \varphi_1 \\ V_{By} &= (\omega_2 (l_1 \cos \theta_1) \sin \varphi_1) - \omega_1 (l_1 \sin \theta_1 \cos \varphi_1) \\ V_{Bz} &= (-l_1 \omega_2 \sin \theta_1 (\sin \varphi_1)^2 + l_1 \omega_2 \sin \theta_1 (\cos \varphi_1)^2) \end{aligned} \quad (26)$$

$$V_C = V_B + \omega_{BC} x r_{C/B} \quad (27)$$

$$r_{C/B} = (l_2 \sin \theta_2 \cos \varphi_2) i - (l_2 \sin \theta_2 \sin \varphi_2) j + (l_2 \sin \theta_2) k \quad (28)$$

$$\omega_{BC} = \omega_4 \sin \varphi_3 i - \omega_4 \cos \varphi_3 j + \omega_3 k \quad (29)$$

$$\omega_{BC} x r_{C/B} = \begin{vmatrix} & i & j & k \\ \omega_4 \sin \varphi_3 & & & \omega_3 \\ l_2 \sin \theta_3 \cos \varphi_3 & l_2 \sin \theta_3 \sin \varphi_3 & l_2 \sin \theta_3 & \end{vmatrix} \quad (30)$$

$$= (\omega_3 (l_2 \cos \theta_3)) i - (\omega_4 (l_2 \sin \theta_4) - \omega_3 (l_2 \sin \varphi_3)) j - (\omega_4 (l_2 \cos \theta_3)) k \quad (31)$$

$$\begin{aligned} V_{Cx} &= (\omega_4 (l_2 \cos \theta_2) \cos \varphi_2) + l_2 \omega_3 \sin \theta_2 \sin \varphi_2 \\ V_{Cy} &= (\omega_4 (l_2 \cos \theta_2) \sin \varphi_2) - \omega_3 (l_2 \sin \theta_2 \sin \varphi_2) \\ V_{Cz} &= (-l_2 \omega_4 \sin \theta_2 (\sin \varphi_2)^2 - (l_2 \omega_4 \sin \theta_2) (\cos \varphi_2)^2) \end{aligned} \quad (32)$$

These six equations allow us to generate a matrix of the kinematic relations between each of the six directional velocities to the four-theta angles, shown in Fig. 23. In Bond graph notation, this concept yields the use of multiport MTF elements, which relate velocities and angular velocities, or forces to torques. These matrix transformations are shown in the set of matrices relating the above equations and are shown in Fig. 24. A bond graph was generated using this matrix consisting of four ‘‘I’’ elements on the left, rotational inertias (for the four angles), and six ‘‘I’’ elements on the right (for the six directional positions). Such bond graph is show in Fig. 25. What the reader can clearly see is that we have a complicated system with four I elements in integral causality on the left (rotational) and six I elements in derivative causality on the right (translational velocities). What to do now?

In [10] (Granda 2003) presents an automated solution for systems with derivative causality. The Granda method is found also in [1] uses matrix operation in symbolic form. It consists of a new set of state space symbolic matrices, which effectively combine the elements in derivative causality symbolically and produce a new set of state space matrices free of derivatives on the right hand side.

A) Derivative Causality State Space Form Solution

The normal explicitly set of differential equations in State Space Form has the following matrix form:

$$\{\dot{x}\} = [A] \{x\} + [B] \{u\} \quad (33)$$

$$\{y\} = [C] \{x\} + [D] \{u\} \quad (34)$$

$$\begin{bmatrix} \dot{x}_1 \\ \dot{y}_1 \\ \dot{z}_1 \\ \dot{x}_2 \\ \dot{y}_2 \\ \dot{z}_2 \end{bmatrix} = \begin{bmatrix} l_1 \sin \theta_1 \sin \varphi_1 & ((l_1 \cos \theta_1) \cos \varphi_1) & 0 & 0 \\ (l_1 \sin \theta_1 \cos \varphi_1) & (l_1 \cos \theta_1 \sin \varphi_1) & 0 & 0 \\ 0 & (-l_1 \omega_2 \sin \theta_1 (\sin \varphi_1)^2 - (l_1 \omega_2 \sin \theta_1) (\cos \varphi_1)^2) & 0 & 0 \\ l_1 \omega_1 \sin \theta_1 \sin \varphi_1 & ((l_1 \cos \theta_1) \cos \varphi_1) & l_2 \sin \theta_2 \sin \varphi_2 & ((l_2 \cos \theta_2) \cos \varphi_2) \\ l_1 \sin \theta_1 & (l_1 \cos \theta_1 \sin \varphi_1) & (l_2 \sin \theta_2 \cos \varphi_2) & (l_2 \cos \theta_2 \sin \varphi_2) \\ 0 & (-l_1 \omega_2 \sin \theta_1 (\sin \varphi_1)^2 - (l_1 \omega_2 \sin \theta_1) (\cos \varphi_1)^2) & 0 & (-l_2 \omega_4 \sin \theta_2 (\sin \varphi_2)^2 - (l_2 \omega_4 \sin \theta_2) (\cos \varphi_2)^2) \end{bmatrix} \begin{bmatrix} \dot{\theta}_1 \\ \dot{\theta}_2 \\ \dot{\theta}_3 \\ \dot{\theta}_4 \end{bmatrix}$$

Fig. 24 Velocities relation to the rotational angles.

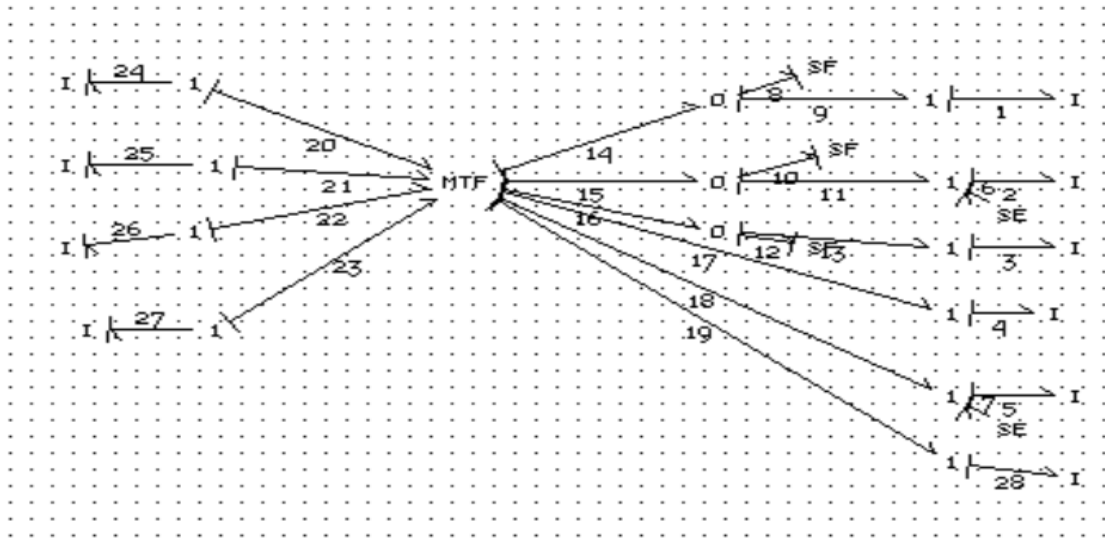


Fig. 25 3-D double pendulum in derivative causality form

The matrices A, B, C, D are the system matrices, $\{x\}$ is the state variables vector, $\{y\}$ is the vector of outputs and $\{u\}$ that of the inputs. The equations that come from the bond graph presented in Fig. 25 do not have the form of equations (33) and (34) exactly. The right hand side contains derivatives. In this particular case six derivatives of the momentums of the I elements of bonds 1, 2, 3, 4, 5, and 28.

The method proposed first in [10] (Granda 2003) and in [1] (Granda JJ, Nguyen L, Carlson T, Brocker S, Sahragard-Monfared G, Fornalski E, 2016) is now expanded and applied to the subject space vehicle. It has the objective to transform the system of equations in implicit form to the state space form of equations (33) and (34), thus eliminating the need to solve an implicit set of equations. If we process the bond graph of Fig. 25, we will obtain a system of equations in the following form.

$$\{\dot{x}\} = [A]\{x\} + [B]\{u\} + [E]\{\dot{x}_d\} \quad (35)$$

$$\{\dot{x}_d\} = [F]\{\dot{x}\} \quad (36)$$

Where the matrix [E] is the corresponding matrix of dependent derivatives and $\{\dot{x}_d\}$ is a vector of dependent derivatives. {F} is a matrix, which establishes a static algebraic dependent relationship between the dependent variable derivatives and the derivatives of the states $\{\dot{x}_d\}$. These relations are the ones that CAMPG produces automatically and thus also its correspondent derivatives relation. Therefore, the system with derivative causality can be expressed as:

$$\{\dot{x}\} = [A]\{x\} + [B]\{u\} + [E]*[F]\{\dot{x}\} \quad (37)$$

Thus

$$[I]\{\dot{x}\} - [E]*[F]\{\dot{x}\} = [A]\{x\} + [B]\{u\} \quad (38)$$

$$[I - E * F] \{\dot{x}\} = [A] \{x\} + [B] \{u\} \quad (39)$$

$$\{\dot{x}\} = [I - E * F]^{-1} [A] \{x\} + [I - E * F]^{-1} [B] \{u\} \quad (40)$$

It is obvious that after these matrix operations, a new state space form emerges which is now in explicit form but with new matrices. The new explicit state space is:

$$\{\dot{x}\} = [A_{new}] \{x\} + [B_{new}] \{u\} \quad (41)$$

$$\{y\} = [C] \{x\} + [D] \{u\} \quad (42)$$

Where:

$$\begin{aligned} [A_{new}] &= [I - E * F]^{-1} [A] \quad \text{and} \\ [B_{new}] &= [I - E * F]^{-1} [B] \end{aligned} \quad (43)$$

This approach generates new A and B matrices for the state-space equations of the system, which can then be used to calculate the derivatives as a normal explicit State Space model in MATLAB. It is obvious that the [10] (Granda J, 2003) approach allows calculating all the state variables.

Respect to the C and D matrices, it depends whether the outputs $\{y\}$ may have derivatives on the right hand side. In this case, the method follows the same logic as shown above for the A and B matrices. So now the equations for the outputs with dependent derivatives on the right hand side are:

$$\{y\} = [C] \{x\} + [D] \{u\} + [G] \{\dot{x}_d\} \quad (44)$$

$$\{\dot{x}_d\} = [H] \{\dot{x}\} \quad (45)$$

Therefore

$$\{y\} = [C] \{x\} + [D] \{u\} + [G][H] \{\dot{x}\} \quad (46)$$

$$\{\dot{x}\} = [I - E * F]^{-1} [A] \{x\} + [I - E * F]^{-1} [B] \{u\}$$

$$\begin{aligned} \{y\} &= [C] \{x\} + [D] \{u\} \\ &\quad + [G * H][I - E * F]^{-1} [A] \{x\} \\ &\quad + [G * H][I - E * F]^{-1} [B] \{u\} \end{aligned} \quad (47)$$

$$\begin{aligned} \{y\} &= [C] \{x\} + [G * H][I - E * F]^{-1} [A] \{x\} \\ &\quad + [D] \{u\} + [G * H][I - E * F]^{-1} [B] \{u\} \end{aligned} \quad (48)$$

$$\begin{aligned} \{y\} &= ([C] + [G * H][I - E * F]^{-1} [A]) \{x\} \\ &\quad + ([D] + [G * H][I - E * F]^{-1} [B]) \{u\} \end{aligned} \quad (49)$$

Therefore

$$\begin{aligned} [C_{new}] &= ([C] + [G * H][I - E * F]^{-1} [A]) \text{ and} \\ [D_{new}] &= ([D] + [G * H][I - E * F]^{-1} [B]) \end{aligned} \quad (50)$$

The A new and B new matrices also provide the appropriate new combined kinematic relations that yield the new time dependent coefficients of the MTF elements which change at each time step. The C_{new} and the D_{new} new matrices complete this new set of explicit symbolic equations which resolves the derivative causality problem.

$$\begin{aligned} \{\dot{x}\} &= [A_{new}] \{x\} + [B_{new}] \{u\} \\ \{y\} &= [C_{new}] \{x\} + [D_{new}] \{u\} \end{aligned} \quad (51)$$

Using the new A, B, C, D matrices the simulation in MATLAB is that of a normal explicit state space form set of first order differential equations and that for the outputs without dependent derivatives.

VI. CONCLUSIONS

The main emphasis of the paper is to present the use of relaxed constraints on a kinematic link set in order to produce an explicit set of differential equations. In order to achieve this the relaxed constraints are shown and their relation to Lagrange multipliers. It has been established the fundamental principles upon which the two and three-dimensional models of the Morpheus vehicle slosh study can be represented by two and three dimensional pendulum models. The use of Lagrange multipliers increased the number of degrees of freedom but produced a set of explicit algebraic and differential equations.

If the problem is to be addressed keeping the dependencies and producing an implicit set of equations in derivative causality, the Granda method using matrix operations can be used to produce automatically a set of explicit equations by producing a new set of state space matrices. Bond Graph models used in conjunction with Lagrange's equations provide a powerful and useful means of simulating complex dynamic systems. The Morpheus project provided a good opportunity to demonstrate this. Simulation data depicting the movements of the Lander were obtained.

VII. REFERENCES

1. Granda JJ, Nguyen L, Carlson T, Brocker S, Sahragard-Monfared G, Fornalski E. "Morpheus Plane-tary Lander Liquid Propellant Fluid Slosh Modeling and Simulation Methods" 12th International Conference on Bond Graph Modeling and Simulation (ICBGM'2016) Montreal, Canada , July 2016.
2. CAMPG (Computer Aided Modeling Program). Cadsim Engineering 2018. <http://www.bondgraph.net>
3. NASA JSC. Project Morpheus "About Morpheus." <http://Morpheuslander.jsc.nasa.gov/about/>
4. Karnopp, D, and D. L. Margolis, and R. C. Rosenberg. "Multibody Systems." *System Dynamics: Modeling, Simulation, and Control of Mechatronic Systems*. Hoboken, NJ: Wiley, 2012.
5. Steuard Jensen. "An Introduction to Lagrange Multipliers,2004-15" <http://www.slimy.com/~steuard/teaching/tutorials/Lagrange.html>
6. Khulief, Yehia A. "Constrained Lagrangian Formulation for Multibody Systems using Bond Graphs", JSME International Journal Series C 34(3):362-369. 1991.
7. Seto, W.. "*Mechanical Vibrations: Schaums Outline of Theory and Problems*". New York, 1964.
8. Karnopp D. "Bond graphs and Lagrange Equations as Aids in Analytical Studies of Electro-Mechanical Systems.
9. Fitzpatrick, R. "Spherical Pendulum." March 3, 2011. From URL: Farside.ph.utexas.edu/teaching/336k/newtonhtml/nodes82.html
10. Granda J. "The CAMP-G/MATLAB-SIMULINK Computer Generated Solution of Bond Graph Derivative Causality". Proceedings of the International Conference on Bond Graph Modeling and Simulation ICBGM 2003. Orlando, Fla. January 2003.

About the authors

Jose J. Granda, PhD, is a Professor of Mechanical Engineering at the California State University in Sacramento, California. He obtained his M.S, and Ph.D. degrees in Mechanical Engineering from the University of California, Berkeley and Davis respectively. He has dedicated his career to research methods to make computer simulations automated and easier for engineers. His expertise in modeling and simulation of space and ground vehicles using computer simulations, vehicle dynamics and vehicle design has been very successful. He is a Professional Registered Mechanical Engineer in the state of California. He received the Distinguished Alumni Award from the University of California, Davis and the Outstanding Research Scholar Award from the California State University, Sacramento. Since 2002, he works with NASA as a NASA Faculty Fellow. Prof. Granda was a NASA spokesperson for 17 missions of the Space Shuttle program. He has served as General Chair or Program Chair of the ICBGM conferences since 1993.

Louis Nguyen. Is an engineer at the NASA Johnson Space Center in Houston, Texas, in the Aerosciences and Flight Mechanics Division. He is the Technical Discipline Lead in dynamics and control, in the Integrated Navigation, Guidance and Control Analysis Branch. He has more than twenty-five years of experience in spacecraft dynamics and control and simulation analysis, supporting the Space Shuttle Program, the International Space Station Program, and other GN&C projects at NASA Johnson Space Center.

Paul Brocker. Is a graduate student in the Mechanical Engineering Department at the California State University, Sacramento. He is supported by the California Space Grant.

Acknowledgement. The authors recognize and thank the California Space Grant Consortium for providing funding for supporting students to become NASA's Workforce of the Future and to keep them motivated to achieve the highest goals.